SUPPLEMEMTAL EXPERIMENTAL PROCEDURES

Compartmentalized Neuronal Culture

All reagents were from Life Technologies (Carlsbad, CA) unless otherwise noted. Primary hippocampal neurons were prepared from embryonic day 18 rat embryos as described (Banker and Goslin, 1998). To apply oligomeric Aβ, inhibitors, or siRNA specifically to distal axons without affecting the cell bodies, the neurons were grown in tripartite microfluidic chambers with two 200-µm-long microgrooves (Hengst et al., 2009; Taylor et al., 2005). Microfluidic chambers were produced according to published protocols (Desai et al., 2009; Park et al., 2006). Neurons (50,000-60,000 per chamber) were cultured on 0.1 mg ml^{-1} poly-D-lysine (Sigma-Aldrich, St. Louis, MO) and 2 µg ml^{-1} laminin (Trevigen, Gaithersburg, MD) coated substrates in Neurobasal medium containing 10% fetal bovine serum and 100 mM glutamine. After 1 DIV the medium was changed to Neurobasal supplemented with 1x B27 and 100 mM glutamine, and half of this medium was replaced with fresh medium after 5 DIV. All experiments were performed at 9-10 DIV. Whenever stated, the axonal or cell body compartments were treated with 3 µM Aβ peptides (oligomeric preparation), 10 µM anisomycin, 500 nM emetine, 30 µM ciliobrevin A (Firestone et al., 2012), 10 µM EHNA (Penningroth et al., 1982), 10 µg ml^{-1} tunicamycin, or 1 µM thapsigargin (Sigma-Aldrich).

Oligomeric Aβ Preparation

Soluble oligomeric Aβ was prepared as described (Stine et al., 2003). Synthetic $Aβ_{1-42}$ peptides (purchased from Dr. D. Teplow, UCLA) were dissolved to 1 mM in hexafluoroisopropanol, aliquoted and dried. The peptides were resuspended to 1 mM in DMSO by bath sonication for 10 min. For oligomer formation, the peptides were diluted to 100 µM in PBS, incubated overnight at 4°C and used on the same day. A scrambled $Aβ_{1-42}$ peptide and an $Aβ_{1-40}$ peptide (American Peptide, Sunnyvale, CA) were treated the same way and used as controls.

Axonal fragmentation measurements

Tubulin fragmentation was measured with ImageJ software (NIH, Bethesda, MD) based on Vohra et al. (2010). Similar criteria were applied when measuring ChAT-positive features in the mouse brain except that the area of continuous particles was analyzed in this case. Particles with high circularity (0.5-1) were not included in order to avoid overestimation of features that could be a result of synaptic retraction and/or axonal fragmentation.

Cell Death and Survival Assays

TUNEL was performed on fixed samples according to manufacturer's instructions (DeadEnd fluorometric TUNEL System, Promega, Madison, WI). Nuclei were counterstained with DAPI. TUNEL-positive nuclei were scored in 5 fields proximal and 5 fields distal to the microgrooves. Survival was analyzed using Calcein staining in living cells. Cell bodies were incubated with 4.17 µg ml^{-1} Calcein AM dye in DMSO for 40-60 min at 37°C. Calcein was quenched with 15 mg ml^{-1} bovine hemoglobin (Sigma-Aldrich). Nuclei were labeled with Hoechst stain. Cells were imaged under live cell conditions inside an incubation chamber at 37°C, 5% CO_2. Positive cells were scored in 5 fields proximal to the microgrooves.

Immunocytochemistry

Neurons grown in microfluidic chambers for 9-10 DIV were fixed for 20 min at room temperature in 4% paraformaldehyde, 4% sucrose in PBS (pH 7.4). Cells were washed several times with PBS, permeabilized and blocked with 3 mg ml^{-1} BSA, 100 mM glycine and 0.25 % Triton X-100. Samples were incubated overnight at 4°C with primary antibodies against 4EBP1, p-4EBP1, S6, p-S6, eIF2α, p-eIF2α, CHOP (1:1,000, Cell Signaling Technology, Danvers, MA), βIII tubulin (1:1,000, Rockland Immunochemicals, Gilbertsville, PA), oligomeric Aβ (NU-4 antibody, 1 µg ml^{-1}, generous gift by Dr. William Klein, Northwestern University) (Lambert et al., 2007), or ATF4 (1:1,000, Abcam, Cambridge, MA). Neurons were washed several times with PBS and incubated for 1 h at room temperature with fluorophore-conjugated Alexa secondary antibodies

(1:200). Samples were mounted with ProLong Gold antifade reagent and imaged using an EC Plan-Neofluar 40x/1.3 objective on an Axio-Observer.Z1 microscope equipped with an AxioCam MRm Rev. 3 camera (Zeiss, Thornwood, NY).

Image acquisition, fluorescence quantification and image processing

The settings for image acquisition of stained axons were determined automatically on a random axonal field of a control sample, ensuring pixel intensities were within the linear range and avoiding pixel saturation using AxioVision acquisition software (Zeiss). The settings were kept the same for all samples in any given experiment. Focusing was performed on the counterstain to ensure blind acquisition of the staining of interest. Images were taken in 5 random axonal field and 3 stacks were imaged per field. Images were quantified generating an automatic mask on the counterstain that established the region of interest (ROI, total axonal area). Pixel intensity within the ROI was measured in all channels using the AxioVision automatic measurement tool**.** Background pixel intensity was calculated in an area outside the ROI. After background substraction the summed mean pixel intensity per area was calculated. Similar prodecures were followed when imaging cell bodies or mouse brains, adjusting the number of stacks to the sample requirement. For presentation in figures the greyscale images were coverted to RGB and contrast and background settings were set the same in control and experimental conditions. Images shown are insets of the axonal fields that best represent the average response of axons.

Bioorthogonal Noncanonical Amino Acid Tagging (BONCAT)

Hippocampal neurons were grown in microfluidic chambers for 9-10 DIV. The culture medium was replaced with methionine-free DMEM for 30 min before the axonal and/or the cell body compartments were incubated with 0.5 mM methionine or the noncanonical amino acid AHA for 1 h at 37°C (Dieterich et al., 2006). Incorporated AHA was labeled with 50 µM fluorescently labeled 488-DBCO (Click Chemistry Tools, Scottsdale, AZ) or -DIBO for 1 h at 37°C through a

copper-free cycloaddition reaction (Ning et al., 2008). Cells were washed twice with fresh methionine-free DMEM medium and twice with PBS. Samples were fixed and counterstained with an anti-βIII antibody as described above.

Retrograde Transport Analysis

To test the efficiency of retrograde transport inhibitors lysosome movement was analyzed using time-lapse fluorescent microscopy. Hippocampal neurons were grown in microfluidic chambers for 9-10 DIV. Axons were incubated with 50 nM Lysotracker Green for 20 min and imaged at 37°C, 5% CO_2. Each axonal field was observed for 4 min taking images every 20 s.

RNA sequencing and Transcriptome Analysis

RNA sequencing was performed using RNA purified from the cell body and axonal compartments of microfluidic chambers using the PrepEase RNA isolation kit (Affymetrix, Santa Clara, CA) and concentrated with RNeasy MinElute Cleanup kit (Qiagen, Valencia, CA). Axons were exclusively treated for 24 h with $A\beta_{1\text{-}42}$ or vehicle at 9-10 DIV. cDNA libraries were created from total RNA using the TruSeq RNA Sample Preparation Kit (Illumina, San Diego, CA). Sequencing was performed on an Illumina MiSeq instrument (paired-end, 2x 150 bp) with biological replicates. Reads were aligned to the rat genome (Rn5) using Tophat 2 (Kim et al., 2013), mapped reads were counted using the summarizeOverlaps function of the GenomicAlignments package (Lawrence et al., 2013), and differential mRNA localization was determined using DESeq2 (Love et al., 2014).

Fluorescent *In Situ* Hybridization (FISH)

Antisense riboprobes were transcribed *in vitro* from sense oligonucleotides using the MEGAshortscript kit with digoxigenin-labeled UTP (Roche Applied Sciences, Indianapolis, IN) according to manufacturer's instructions. Five non-overlapping probes recognizing *Egfp* (negative control) or *Atf4* mRNA were used for each FISH staining. All sense oligonucleotides

used were transcribed using a T7 promoter site (...GCCCTATAGTGAGTCGTATTAC-3') at the 3’ end.

Egfp.1, 5’-GATGCCACCTACGGCAAGCTGACCCTGAAGTTCATCTGCACCACCGGCAAG…

Egfp.2, 5’-GACCACATGAAGCAGCACGACTTCTTCAAGTCCGCCATGCCCGAAGGCTAG…

Egfp.3, 5’-ACTTCAAGGAGGACGGCAACATCCTGGGGCACAAGCTGGAGTACAACTACG…

Egfp.4, 5’-AAGCAGAAGAACGGCATCAAGGTGAACTTCAAGATCCGCCACAACATCGAG…

Egfp.5, 5’-AGTTCGTGACCGCCGCCGGGATCACTCTCGGCATGGACGAGCTGTACAAGG…

Atf4.1, 5’-AGCCCCTCAGACAGTGAACCCAATTGGCCATCTCCCAGAAAGTGTAATA…

Atf4.2, 5’-GTTAAGCACATTCCTCGATACCAGCAAATCCCTACAACATGACCGAGATG…

Atf4.3, 5’-AAGGAGGAAGACACTCCCTCTGATAGTGACAGTGGCATCTGTATGAGCCC…

Atf4.4, 5’-CTTAGATGACTATCTGGAGGTGGCCAAGCACTTCAAACCTTCATGGGTTCT…

Atf4.5, 5’-AACGAGGCTCTGAAAGAGAAGGCAGATTCTCTCGCCAAAGAGATTCAGTA…

FISH was performed as previously described (Hengst et al., 2009). The samples were incubated with a total of 125 ng of digoxigenin-labeled riboprobe (25 ng each) in 25 µl hybridization buffer overnight at 37°C. After washing, cells were incubated with anti-digoxin (1:500, Sigma-Aldrich) and anti-βIII tubulin antibodies overnight at 4°C. Cells were washed several times with TBST and further incubated with fluorophore-conjugated Alexa secondary antibodies.

Real time RT-PCR

Total RNA from the cell bodies and the axonal compartments was isolated and concentrated as above. A total amount of approximately 2 ng was generally isolated from axonal lysates and 10 µl of concentrated RNA were used for reverse transcription. In the case of the total RNA from cell bodies, 100 ng were reverse transcribed. Reverse transcription was performed using SuperScript III First-Strand Synthesis SuperMix for qRT-PCR following manufacturer’s instructions. cDNA was pre-amplified using the TaqMan PreAmp Kit according to

manufacturer's instructions using the following conditions: an initial denaturation step at 95℃for 10 min, followed by 14 cycles of denaturation at 95℃for 15 sec and annealing/extension at 60℃ for 4 min. Real time RT-PCR was performed with TaqMan Gene Expression master mix in a StepOnePlus Real-Time PCR instrument using the following conditions: an initial denaturation step at 95℃for 10 min, followed by 40 cycles of denaturation at 95℃for 15 s and extension at 60℃for 1 min. The *Atf4* gene expression set (Rn00824644_g1) was used. Gene expression was normalized to input RNA.

siRNA Transfection

Hippocampal neurons were grown in microfluidic chambers 8-9 DIV and axons were exclusively transfected with siRNAs using NeuroPORTER (Genlantis, San Diego, CA) following manufacturer's instructions with minor modifications. Briefly, a mix containing 100 nM siRNA and 10% NeuroPORTER in serum- and antibiotic-free medium was added to the axonal compartment. 2 h after transfection the axonal compartments were supplemented with an equal volume of Neurobasal medium containing 2x B27 and 100 nM glutamine. Similar procedures were followed when transfecting the cell body compartment. The final siRNA concentration was 50 nM. 24 h after the transfection, axons were treated with vehicle or $A\beta_{1\text{-}42}$.
Control siRNA; sequence, 5'-CCCUUCGUUCCUUCCAAUCUGUCCA-3'; complementary, 5'-UGGACAGAUUGGAAGGAACGAAGGG-3'; *Atf4* siRNA 1; sequence, 5'-AACCCAUGAGGUUUGAAGAGCUUGG-3'; complementary; 5'-CCAAGCACUUCAAACCUCAUGGGUU-3'; *Atf4* siRNA 2; sequence, 5'-AUAAGCAGCAGAGUCAGGUUCCUA-3'; complementary, 5'-UAGGAAGCCUGACUCUGCUGCUUAU-3'. *Chop* siRNA; sequence, 5'-AACAGUUCAUGCUUGGUGCAGACUG-3'; complementary, 5'-CAGUCUGCACCAAGCAUGAACUGUU-3'.

siRNA sequences were selected based on the knockdown efficiency predicted by BLOCK-IT™ RNAi designer and the minimum off-target effects predicted by BLAST (E value ~10^{-6} for expected target sequences).

Immunoblot Analysis

Immunoblots were performed using antibodies against p-4EBP1, p-S6, pS6K, ATF4 (all 1:1,00), β-actin (1:10,000, Millipore, Billerica, MA), and HRP-conjugated secondary antibodies (Pierce Biotechnology, Rockford, Il) and visualized with SuperSignal West Pico Chemiluminescent Substrate (Pierce).

Luciferase Assay

Hippocampal neurons were grown in microfluidic chambers for 8-9 DIV and cell bodies were transfected using NeuroPORTER with 200 ng of a pNL vector containing the coding sequence of Firefly luciferase under the control of an ATF4 response element (Promega) or an ATF6 response element (Addgene, Cambridge, MA) (Wang et al., 2000) and 20 ng of a PGL4 vector containing the coding sequence of Renilla luciferase under the control of the CMV promoter (Promega). 24 h after transfection axons were treated with vehicle or $A\beta_{1-42}$ in the presence or absence of inhibitors or siRNAs. Relative Firefly luciferase activity was measured 24 or 48 h after the treatments using the Dual-Luciferase Reporter Assay System (Promega) following manufacturer's instructions. Background was established measuring luminescence in untransfected cells.

***In vivo* Injection Experiments**

National and institutional guidelines for the care and use of laboratory animals were followed for all mouse experimentation. Stereotaxic injections were performed according to Sotthibundhu et al. (2008) with minor modifications (Jean et al., 2013). 9-12-month-old C57Bl/6J mice (Jackson Laboratory, Bar Harbor, ME) were anesthetized with ketamine (95 mg per kg of body mass) and

xylazine (7 mg per kg of body mass), and then placed in a stereotaxic frame (Stoelting, Wood Dale, IL). Stereotaxic injections were conducted using convection-enhanced delivery at a rate of 0.5 µl min^{-1} using the Quintessential Stereotaxic Injector (Stoelting) at the following coordinates measured from bregma: anterior-posterior, -2.00 mm; medial-lateral, ±1.3 mm (right or left DG, respectively); dorsal-ventral, -2.2 mm. Mice were injected with 4 µl vehicle into the left DG and 4 µl oligomeric $A\beta_{1-42}$ (100 µM in PBS) into the right DG. Based on the observed spread of $A\beta_{1-42}$ we estimate a final $A\beta_{1-42}$ concentration of ~30 nM in the DG. For siRNA experiments, 4 µl $A\beta_{1-42}$ and 20 µg of siRNA were co-injected (control siRNA left DG, *Atf4* siRNA right DG). A 2% suspension of the retrograde label fluorogold (Fluorochrome, LLC, Denver, CO) was co-injected in all cases. Animals were sacrificed 2, 4 or 7 DPI by anesthesia with ketamine and xylazine followed by transcardial perfusion with 4% paraformaldehyde in PBS. Brains were post-fixed in 4% paraformaldehyde for 24 h at 4°C, followed by 30% sucrose infiltration, embedded in Tissue-Tek O.C.T Compound (Sakura Finetek, Torrance, CA), and cryostatically sectioned at 20 µm thickness. *Atf4* siRNA: sequence, 5'-CCAAGCACUUGAAACCUCAUGGGUU-3'; complementary, 5'-AACCCAUGAGGUUUCAAGUGCUUGG-3'.

RNAscope *in situ* hybridization on brain sections

2-7 DPI, detection of *Atf4* mRNA in the DG was performed using the RNAscope Multiplex Fluorescent Reagent Kit (Wang et al., 2012) (Advanced Cell Diagnostics, Hayward, CA) according to manufacturer's instructions with minor modifications. After ethanol dehydration, slices were heated in 10 mM sodium citrate (pH 6), 0.05% Tween 20 for epitope retrieval. No proteinase K treatment was performed. Background fluorescence was established with an RNAscope negative probe whereas *Atf4* detection was performed using a specific *Atf4*-targeting probe set targeting residues 20-1381 of the mouse *Atf4* mRNA (NM_009716). Following *in situ* hybridization, brain slices were blocked with 3 mg ml^{-1} BSA, 100 mM glycine and 0.25% Triton X-100 and incubated with an anti-ChAT antibody (1:100, Millipore) for 2 days at 4°C. After

several washes slices were incubated with secondary antibodies, nuclei were counterstained with DAPI, and samples were mounted with ProLong Gold mounting medium.

Immunohistochemistry and TUNEL on brain sections

Brain slices were heated in 10 mM sodium citrate (pH 6), 0.05% Tween 20 for epitope retrieval, washed several times with PBS, and blocked and permeabilized with 3% BSA, 100 mM glycine and 0.25% Triton X-100 for 1 h at room temperature. Brain slices were incubated with primary antibodies against oligomeric $A\beta_{1-42}$ (NU-4, 1 µg ml^{-1}), ChAT (1:100), p-S6 (1:1,000), ATF4 (1:1,000), CHOP (1:1,000), and NeuN (1:500, Millipore). All primary antibodies were incubated overnight at 4°C, except for ChAT staining, which was performed for 2 days. No epitope retrieval was performed for the detection of oligomeric $A\beta_{1-42}$. Primary antibodies were detected with a fluorescently labeled secondary antibody and, when indicated, nuclei were counterstained with DAPI.

Determination of cell numbers in brain sections / stereology

Brain slices were randomly selected from serial sections for staining and quantification. Two series typically containing 8 brain slices equally spaced (120 □m) covering the anterior basal forebrain were randomly chosen. Because of the density (except for NeuN positive neurons) generally all cells within the region of interest defined by fluorogold staining were quantified based on Sotthibundhu et al. (2008). For selected experiments cells were quantified using the optical dissector method with the Stereo Investigator software (MBF Bioscience, Williston, VT). The region of interest was again defined with the help of fluorogold staining. For systematic sampling of ChAT-positive neurons the frame area was set to 10,000 □m^2 with a sampling interval of 100 □m on the x- and y-axis. In the case of NeuN-positive cells the frame area was set to 5,625 □m^2 with a sampling interval of 350 □m on the x- and y-axis. In both cases the optical dissector height was set to a 10 □m fraction of the section thickness (15-18 □m after

processing) and the safe guard zone was 2 □m in the upper and lower limits. In all brain samples, the orientation of the counting grids was randomized.

Human Brain Samples

Autopsy case material was obtained through the New York Brain Bank at Columbia University. AD neuropathological changes were assessed using the CERAD protocol (Mirra et al., 1991), Braak neurofibrillary tangle staging (Braak et al., 1993) and the NIA Reagan consensus criteria (—, 1997). Cerebral amyloid angiopathy was assessed according to the Vonsattel criteria (Greenberg and Vonsattel, 1997). Paraffin-embedded sections (8 µm thickness) were obtained from the mesial temporal lobe at the level of the lateral geniculate body from eight AD and eight non-demented age and sex matched controls.

#	*Classification*	*Age*	*Sex*	*Braak NFT stage*	*CERAD plaque score*	*Amyloid angiopathy*	*NIAR*	*PMI (min)*
1	Control	74	M	II	None	0	0	255
2	Control	74	M	III	None	0	0	93
3	Control	79	W	III	None	0	0	180
4	Control	87	M	III	Sparse	0	Low	310
5	Control	90	M	III	Sparse	0	Low	270
6	Control	74	M	IV	Sparse	0	Low	180
7	Control	80	M	II	Sparse	+	Low	115
8	Control	89	M	IV	Sparse	+	Low	942
9	Moderate AD	83	M	V	Moderate	0	Intermediate	695
10	Moderate AD	84	M	V	Moderate	++	Intermediate	264
11	Moderate AD	85	W	V	Moderate	+	Intermediate	253
12	Moderate AD	98	M	V	Moderate	0	Intermediate	144
13	Severe AD	75	M	VI	Frequent	++	High	295
14	Severe AD	82	M	VI	Frequent	+	High	127
15	Severe AD	86	M	VI	Frequent	++	High	260
16	Severe AD	89	W	VI	Frequent	++	High	320

NFT, neurofibrillary tangle; CERAD, Consortium to establish a registry for Alzheimer disease; NIAR, National Institute on Aging-Reagan criteria; PMI, post mortem interval

RNAscope *in situ* hybridization was performed following the manufacture's protocol. Background staining was established with an RNAscope negative probe whereas *Atf4* detection was performed using a specific *Atf4*-targeting probe set targeting residues 15-1256 of the human *Atf4* mRNA (NM_001675.2). Before samples were counterstained, the presence of *Atf4*

positive granules was verified under the microscope. Granules were readily found not only in cell body layers, but also in the neuropil in all cases, suggesting the localization of *Atf4* mRNA to the periphery of the cells. Brain samples were then counterstained with Luxol Fast Blue Cresyl Echt Violet kit (American Mastertech Scientific, Lodi, CA) to visualize axons and with cresyl violet to visualize neuronal bodies. The counterstaining was carefully monitored under the microscope, especially in the case of Luxol Fast Blue, to ensure that the dye would not mask *Atf4* positive granules. After processing, brain samples were analyzed. Immunohistochemical staining was performed using an antiserum to ATF4 (1:200, Santa Cruz Biotechnology, Santa Cruz, CA) and performed on an automated slide staining platform (Ventana Medical Systems, Tucson, AZ). The samples were scored based on the frequency of appearance of *Atf4* mRNA granules or ATF4 protein containing axons or cell bodies. The score ranged from 0 (absent) to 3 (high frequency), regardless of the amount of granules per axon or cell body. Results are plotted as cumulative frequency distributions.

SUPPLEMENTAL FIGURE LEGENDS

Figure S1. Validation of the use of microfluidic chambers to study local protein synthesis in response to $A\beta_{1-42}$. Related to Figure 1.

(A) The effective concentration of Aβ is reduced in microfluidic chambers. Hippocampal neurons were grown normally or in microfluidic devices for 9-10 DIV. All cellular compartments (the somato-dendritic compartment in case of the microfluidic devices) were treated with increasing concentrations of $A\beta_{1-42}$ oligomers for 24 h. Samples were processed for TUNEL. Mean ±SEM of 50-90 microscopy fields per condition (n=5-9 biological replicates per group).

(B) Western blot analysis of molecular markers for active protein synthesis after 24 h of $A\beta_{1-42}$ exposure in all cellular compartments (including cell bodies). Mean ±SEM of 5 biological replicates. *p<0.05.

(C) Neurons grown in microfluidic chambers were immunostained for 4EBP1 and p-4EBP1 after selective treatment of the cell body compartment with vehicle or $A\beta_{1-42}$ oligomers for 24 h. Mean ±SEM of 40 optical fields per condition (n=8 biological replicates per group). **p<0.01. Scale bars, 20 μm (cell body compartment), 10 μm (axonal compartment).

(D) Validation of BONCAT for the visualization of newly synthesized proteins in hippocampal neurons grown in microfluidic devices. Cells were grown in microfluidic chambers for 10 DIV. The different subcellular compartments were incubated in the absence or present of AHA and treated with the indicated compounds. AHA incorporation to proteins was visualized by incubating the cells with 488-DIBO or -DBCO alkyne and is represented in a pseudocolor scale. Mean ±SEM of 24-30 optical fields per condition (n=5-6 biological replicates per group). ***p<0.001. Scale bar, 20 μm.

(E) Hippocampal neurons were cultured in microfluidic chambers and axons were treated with vehicle or $A\beta_{1-42}$ for 24 h. 2 h and 30 min prior to fixation, axons were pre-incubated with emetine or vehicle and then sequentially incubated with AHA and 488-alkyne. Newly

synthesized proteins were detected by their fluorescence signal at 488 nm (represented in pseudo color). Mean ±SEM of 25-35 optical fields per condition (5-7 biological replicates per group). **p<0.01; ***p<0.001. Scale bar, 5 μm.

Figure S2. Validation of cell death assays and retrograde transport in the presence or absence of oligomeric Aβ and the indicated inhibitors. Related to Figure 2.

(A) Hippocampal neurons were cultured in microfluidic chambers for 9-10 DIV and axons were treated with vehicle or $A\beta_{1-42}$ oligomers for 24 h and with vehicle or the indicated compounds for the last 6 h of $A\beta_{1-42}$ exposure. The culture medium from the axonal compartments was then replaced with 50% conditioned medium and cells were allowed to recover. A schematic representation of the experimental approach is shown. Cell death was assessed by TUNEL staining and nuclei were counterstained with DAPI. Mean ±SEM of 40-100 optical fields (n=4-10 biological replicates per group). ***p<0.001. Scale bar, 50 μm.

(B) Effect of retrograde transport inhibitors locally applied to axons on lysosomal movement. Hippocampal neurons were grown in microfluidic chambers for 9-10 DIV and treated with the indicated compounds for 6 h. Lysosomes were stained with Lysotracker Green and lysosomal movement was followed by live microscopy for 4 minutes. Mean ±SEM of 53-118 individual lysosomes per condition (n=4-5 biological replicates per group). ***p<0.001. Scale bars, 5 μm.

(C) Hippocampal neurons were cultured in microfluidic chambers for 9-10 DIV and axons were treated with vehicle or $A\beta_{1-42}$ oligomers for 24 h and the culture medium from the axonal compartments was then replaced with 50% conditioned medium and cells were allowed to recover. 6 h prior to fixation axons were treated with vehicle or EHNA. A schematic representation of the experimental approach is shown. Cell death was assessed by TUNEL staining and nuclei were counterstained with DAPI. Mean ±SEM of 50-60 optical fields (n=5-6 biological replicates per group). ***p<0.001. Scale bar, 50 μm.

(D) Axons of hippocampal neurons were exposed to $A\beta_{1-42}$ oligomers for 24 h in the presence or absence of the indicated compounds. The culture medium from the axonal compartments was replaced with 50% conditioned medium and cells were allowed to recover (see the schematic in Figures 2D and S2A). Cell bodies were stained for oligomeric $A\beta_{1-42}$ and counterstained for tubulin. Very (if any) few cells showed positive staining for $A\beta_{1-42}$ (see also Figure 2C). Note that the uptake of Aβ by cell bodies does not correlate with changes in cell death after axons were exposed to the indicated inhibitors (compare Figures 2D and E, S2A, S2C and S2D). Similar results were found using the experimental approach depicted in Figures 2E and S2C (data not shown). Scale bar, 20 μm.

Figure S3. *Atf4* localization and expression in axons and cell bodies after axonal application of $A\beta_{1-42}$ oligomers and the indicated inhibitors. Related to Figure 3.

(A) The normalized read counts of two transcripts known to be present in both cell bodies and axons (*Actb* and *Tubb3*) (Bassell et al., 1998; Eng et al., 1999), a transcript known to be localized only to dendrites (*Camk2a*) (Burgin et al., 1990) and two non-localized transcripts (*H1f0* and *Hist3h2a*) (Taylor et al., 2005) were compared. Only transcripts with expression values above those for the non-axonal mRNAs were considered significantly localized to axons. These were found in the first decile of our datasets.

(B) Comparison the 10% most highly expressed transcripts in vehicle- and $A\beta_{1-42}$-treated axons. Both RNA populations shared 70% identity, but 775 transcripts were uniquely localized to either of both conditions.

(C) Hippocampal neurons were grown in microfluidic chambers for 9-10 DIV and treated with vehicle or $A\beta_{1-42}$ oligomers for 18 h. 3 h prior to sample processing axons were treated with DMSO, anisomycin or emetine. *Atf4* mRNA levesl were measured by quantitative FISH. Mean ±SEM of 25-30 axonal fields per condition (n=5-6 biological replicates per group). *p<0.05; **p<0.01, ***p<0.001 compared to the negative probe. Scale bar, 5 μm.

(D) Axons of hippocampal neurons were transfected with a control siRNA (ctrl.) or a siRNA targeting *Atf4* 24 h hours before the local exposure to $A\beta_{1-42}$ oligomers. After treating the axons with vehicle or $A\beta_{1-42}$ for 24 h, axonal *Atf4* mRNA levels were analyzed by quantitative FISH. Mean ±SEM of 31-42 axonal fields per condition (n=6-9 biological replicates per group). *p<0.05, ***p<0.001. Scale bar, 5 µm.

(E) Axons of hippocampal neurons were treated as in D. *Atf4* mRNA levels in the cell bodies were analyzed by quantitative FISH. Mean ±SEM of 30-45 axonal fields per condition (n=6-9 biological replicates per group). Scale bar, 20 µm.

(F) Axons of hippocampal neurons were treated as in D. 6 h prior to sample processing, axons were exposed to vehicle or ciliobrevin A. ATF4 protein levels in cell bodies were measured by quantitative immunofluorescence. Mean ±SEM of 35-40 axonal fields per condition (n=7-8 biological replicates per group). Scale bar, 20 µm.

(G) Axons of hippocampal neurons were exposed to vehicle or $A\beta_{1-42}$ oligomers for 24 h. 6 h prior to fixation, axons were treated in the absence or presence of EHNA. Axonal ATF4 protein levels were measured by quantitative immunofluorescence. Mean ±SEM of 27-38 axonal fields per condition (n=5-8 biological replicates per group). *p<0.05; **p<0.01. Scale bar, 10 µm.

(H) Axons of hippocampal neurons were treated as in G. 6 h prior to sample processing axons were incubated with vehicle or ciliobrevin A. *Atf4* mRNA levels were measured by quantitative FISH. Mean ±SEM of 25-30 axonal fields per condition (n=5-6 biological replicates per group). ***p<0.01 compared to the negative probe. Scale bar, 5 µm.

Figure S4. ATF4 and ATF4-related responses in cell bodies. Related to Figure 4.

(A) Validation of the ATF4-RE and p5xATF6-GL3 reporter constructs following ER stress induction in all cellular compartments (including cell bodies). Cell bodies transfected with either ATF4-RE or p5xATF6-GL3 reporter and the CMV-Renilla luciferase reporter construct were

exposed to tunicamycin (TM) or thapsigargin (Tg) for 24 h. Relative normalized Firefly luciferase activity was measured in whole cell lysates. Mean ±SEM of 6-7 biological samples. **p<0.01.

(B) Axons of hippocampal neurons were exposed to vehicle or $A\beta_{1-42}$ oligomers for 24 and 48 h. Expression of ATF4 in the cell body compartment was analyzed by immunoblot. Mean ±SEM of 9-11 biological replicates per condition. $A\beta_{1-42}$ bars are normalized to their associated control bars. * p<0.05.

(C) Axons of hippocampal neurons were exposed to $A\beta_{42scrmabled}$ or $A\beta_{1-40}$ for 48 h. CHOP protein expression in cell bodies was analyzed by quantitative immunofluorescence. Mean ±SEM of 25-30 optical fields (n=5-6 biological replicates per condition). *p<0.05. Scale bar, 20 μm.

(D) Axons of hippocampal neurons were exposed to vehicle or $A\beta_{1-42}$ oligomers and incubated in the presence or absence of the indicated compounds for 6 h. The culture medium in the axonal compartments was the replaced with 50% conditioned medium for 24 h. ATF4 protein levels in cell bodies were analyzed by immunoblot. Mean ±SEM of 12-13 biological replicates per condition. $A\beta_{1-42}$ bars are normalized to their associated control bars. * p<0.05.

(E) Axons of hippocampal neurons were transfected with a control siRNA (ctrl.) or a siRNA targeting *Atf4* 24 h hours before the local exposure to $A\beta_{1-42}$ oligomers. After treating the axons with vehicle or $A\beta_{1-42}$ for 48 h, ATF4 protein levels were analyzed in the somatic compartment by immunoblot. Mean ±SEM of 13-14 biological replicates per condition. $A\beta_{1-42}$ bars are normalized to their associated control bars. * p<0.05.

(F) Axons of hippocampal neurons were treated as in D. To analyze survival levels, cell bodies were stained with Calcein and nuclei were counterstained with Hoechst. Mean ±SEM of 35-40 optical fields per condition (n=7-8 biological replicates per group). *p<0.05. Scale bar, 50 μm.

Figure S5. Effect of $A\beta_{1-42}$ injection in the dentate gyrus (DG). Related to Figure 5.

(A) Schematic representation of a sagittal view of the mouse brain indicating the site of the intra-hippocampal injection (left). Coronal view of a mouse brain in which the effect of oligomeric $A\beta_{1-42}$ in the hippocampal formation (HF) was analyzed,

(B) Co-localization of ChAT and synaptophysin suggests that most cholinergic axons innervate the GCL and, to a lesser extent, the molecular layer (ML) and polymorphic cell layers (PCL) molecular as previously described (Clarke, 1985). Scale bar, 50 µm (10 µm, inset).

(C) Semi-automated quantification of axons using Image J. Note that even if ChAT staining appears more punctate in $A\beta_{1-42}$-injected hemispheres, no major axonal loss was detected. Measurements represent the mean number of axons/axonal structures within 74,740 μm^3 volumetric fractions of the DG. Mean ±SEM of ~4 brain slices per mouse (n=4 mice). Scale bar, 20 µm.

(D) FISH for *Atf4* mRNA in the GCL of mice injected with vehicle and $A\beta_{1-42}$. Axons of cholinergic neurons were identified by ChAT immunostaining. Nuclei were counterstained with DAPI. Scale bar, 20 µm.

(E) p-S6 staining in the GCL of mice injected with vehicle or $A\beta_{1}$-42. Axons were counterstained with ChAT. Scale bar, 20 µm.

(F) ATF4 protein staining in the GCL. Axons were counterstained with ChAT. Scale bar, 20 µm.

(G) Mice were injected with $A\beta_{1-42}$ oligomers in both hemispheres of the brain. The left hemisphere was co-injected with a control (ctrl.) siRNA and the right hemisphere with an *Atf4* siRNA. Presence of *Atf4* mRNA in the GCL. Axons were counterstained with ChAT. Scale bar, 20 µm.

(H) Mice were treated as in F. ATF4 protein in the GCL was detected. Axons were counterstained with ChAT. Scale bar, 20 µm.

(I) Mice were treated as in F. Axonal loss was quantified as in C. Mean ±SEM of ~4 brain slices per mouse (n=4 mice). Scale bar, 20 µm.

Figure S6. Effect of Intra-hippocampal injection of $A\beta_{1-42}$ on neurodegeneration. Related to Figure 6.

(A) Schematic representation of a coronal section of the mouse forebrain brain. Vehicle was injected into the left hemisphere and $A\beta_{1-42}$ into the right hemisphere. The vertical solid black bars indicate the interval of brain sections adjacent to the site of the injection that were selected to analyze the basal fore brain (BF). The hippocampal formation is highlighted in grey and the BF in red. The red solid arrow indicates the projections of basal forebrain cholinergic neurons to the dentate gyrus. MOB, main olfactory bulb; CTX, cortex; CBX, cerebellar cortex; BF, basal forebrain; MSDDB, complex of the medial septum-diagonal band of Broca.

(B) To define the region of the BF were cells projected to the site of the injection, both vehicle and $A\beta_{1-42}$ oligomers were co-injected with the retrograde tracer fluorogold. Representative image of basal forebrain cells (within the NDB) stained with fluorogold. Scale bar, 200 µm.

(C) Following vehicle or $A\beta_{1-42}$ injection (7 DPI) sections neurons of the basal forebrain were immunostained for ATF4 and the pan-neuronal marker NeuN 2 to 7 DPI. Mean ±SEM of ~8 brain slices per mouse (n=4-5 mice). Scale bar, 50 µm.

(D) Following vehicle or $A\beta_{1-42}$ injection (7 DPI), ChAT-positive neurons quantified in both nuclei of the BF (left graph) or separately in the MS and the nucleus of the diagonal band (NDB, right graph) by the optical dissector method. Mean ±SEM of ~8 brain slices per mouse (n=5 mice). **p<0.01.

(E) Following vehicle or $A\beta_{1-42}$ injection (7 DPI), NeuN-positive neurons quantified in both nuclei of the BF (left graph) or separately in the MS and NDB (right graph) by the optical dissector method. Mean ±SEM of ~8 brain slices per mouse (n=5 mice).

(F) Mice were injected with $A\beta_{1-42}$ oligomers in both hemispheres of the brain. The left hemisphere was co-injected with a control (ctrl.) siRNA and the right hemisphere with an *Atf4* siRNA. Quantification of ChAT-positive neurons in the MS and the NDB by the optical dissector method. Mean ±SEM of ~8 brain slices per mouse (n=5 mice).

(G) Following vehicle or $A\beta_{1-42}$ injection (7 DPI), the thickness of the GCL and the presence of TUNEL-positive cells were measured in the DG. Nuclei were counterstained with DAPI. Mean ±SEM of ~8 brain slices per mouse (n=5 mice). **p<0.01. Scale bar, 50 µm.

(H) Mice were treated as in F and brain slices were processed as in G. Mean ±SEM of ~8 brain slices per mouse (n=5 mice). **p<0.01. Scale bar, 50 µm.

(I) Proposed model for $A\beta_{1-42}$-induced, axonally synthesized ATF4-mediated neurodegeneration: $A\beta_{1-42}$ oligomers trigger the axonal recruitment and translation of a discrete set of mRNAs (1), including the p-eIF2α-dependent translation of *Atf4* mRNA (2). Both events likely depend directly on $A\beta_{1-42}$. Once axons have reached a stress threshold, ATF4 protein is transported back to the nucleus (3), where ATF4-dependent transcriptional activation leads to a phenotypic loss of cholinergic neurons and to an induction CHOP (5). CHOP and possibly the loss of phenotype lead to cell death.

Supplemental Table S1. Significantly changed transcripts. Related to Figure 3

Total mRNA was harvested from axons treated with vehicle or $A\beta_{1-42}$ for 24 h. cDNA libraries were created from total RNA and sequenced on an Illumina MiSeq instrument. Paired-end reads were mapped to the rat genome, and expression levels and differential expression was determined with DESeq2. The axonal abundance of 362 mRNAs was significantly changed (Benjamini-Hochberg adjusted p values < 0.1) in $A\beta_{1-42}$-treated axons, of which 211 were down and 151 were upregulated. lfcSE, standard error; stat, Wald statistics; padj, Benjamini-Hochberg adjusted p value.

Supplemental Table S2. Number of TUNEL- and ChAT-positive cells counted. Related to Figure 6

Sections of the basal forebrain of injected mice were processed for TUNEL and ChAT staining. TUNEL-positive (A) and ChAT-positive (B) cells were counted in both nuclei or the MS and NDB

separately. For each analysis five animals were used (indicated by alternating color). Each line indicates an individual section of the BF.

SUPPLEMENTAL REFERENCES

— (1997). Consensus recommendations for the postmortem diagnosis of Alzheimer's disease. The National Institute on Aging, and Reagan Institute Working Group on Diagnostic Criteria for the Neuropathological Assessment of Alzheimer's Disease. Neurobiol Aging *18*, S1-2.

Banker, G., and Goslin, K. (1998). Culturing nerve cells, 2nd edn (Cambridge, Mass.: MIT Press).

Bassell, G.J., Zhang, H., Byrd, A.L., Femino, A.M., Singer, R.H., Taneja, K.L., Lifshitz, L.M., Herman, I.M., and Kosik, K.S. (1998). Sorting of β-actin mRNA and protein to neurites and growth cones in culture. J Neurosci *18*, 251-265.

Braak, H., Braak, E., and Bohl, J. (1993). Staging of Alzheimer-related cortical destruction. Eur Neurol *33*, 403-408.

Burgin, K.E., Waxham, M.N., Rickling, S., Westgate, S.A., Mobley, W.C., and Kelly, P.T. (1990). In situ hybridization histochemistry of Ca^{2+}/calmodulin-dependent protein kinase in developing rat brain. J Neurosci *10*, 1788-1798.

Clarke, D.J. (1985). Cholinergic innervation of the rat dentate gyrus: an immunocytochemical and electron microscopical study. Brain Res *360*, 349-354.

Desai, S.P., Freeman, D.M., and Voldman, J. (2009). Plastic masters-rigid templates for soft lithography. Lab Chip *9*, 1631-1637.

Dieterich, D.C., Link, A.J., Graumann, J., Tirrell, D.A., and Schuman, E.M. (2006). Selective identification of newly synthesized proteins in mammalian cells using bioorthogonal noncanonical amino acid tagging (BONCAT). Proc Natl Acad Sci U S A *103*, 9482-9487.

Eng, H., Lund, K., and Campenot, R.B. (1999). Synthesis of β-tubulin, actin, and other proteins in axons of sympathetic neurons in compartmented cultures. J Neurosci *19*, 1-9.

Firestone, A.J., Weinger, J.S., Maldonado, M., Barlan, K., Langston, L.D., O'Donnell, M., Gelfand, V.I., Kapoor, T.M., and Chen, J.K. (2012). Small-molecule inhibitors of the AAA+ ATPase motor cytoplasmic dynein. Nature *484*, 125-129.

Greenberg, S.M., and Vonsattel, J.P. (1997). Diagnosis of cerebral amyloid angiopathy. Sensitivity and specificity of cortical biopsy. Stroke *28*, 1418-1422.

Hengst, U., Deglincerti, A., Kim, H.J., Jeon, N.L., and Jaffrey, S.R. (2009). Axonal elongation triggered by stimulus-induced local translation of a polarity complex protein. Nat Cell Biol *11*, 1024-1030.

Jean, Y.Y., Ribe, E.M., Pero, M.E., Moskalenko, M., Iqbal, Z., Marks, L.J., Greene, L.A., and Troy, C.M. (2013). Caspase-2 is essential for c-Jun transcriptional activation and Bim induction in neuron death. Biochem J *455*, 15-25.

Kim, D., Pertea, G., Trapnell, C., Pimentel, H., Kelley, R., and Salzberg, S.L. (2013). TopHat2: accurate alignment of transcriptomes in the presence of insertions, deletions and gene fusions. Genome Biol *14*, R36.

Lambert, M.P., Velasco, P.T., Chang, L., Viola, K.L., Fernandez, S., Lacor, P.N., Khuon, D., Gong, Y., Bigio, E.H., Shaw, P.*, et al.* (2007). Monoclonal antibodies that target pathological assemblies of Aβ. J Neurochem *100*, 23-35.

Lawrence, M., Huber, W., Pagès, H., Aboyoun, P., Carlson, M., Gentleman, R., Morgan, M.T., and Carey, V.J. (2013). Software for computing and annotating genomic ranges. PLoS Comput Biol *9*, e1003118.

Love, M.I., Huber, W., and Anders, S. (2014). Moderated estimation of fold change and dispersion for RNA-Seq data with DESeq2. bioRxiv.

Mirra, S.S., Heyman, A., McKeel, D., Sumi, S.M., Crain, B.J., Brownlee, L.M., Vogel, F.S., Hughes, J.P., van Belle, G., and Berg, L. (1991). The Consortium to Establish a Registry for Alzheimer's Disease (CERAD). Part II. Standardization of the neuropathologic assessment of Alzheimer's disease. Neurology *41*, 479-486.

Ning, X., Guo, J., Wolfert, M.A., and Boons, G.J. (2008). Visualizing metabolically labeled glycoconjugates of living cells by copper-free and fast huisgen cycloadditions. Angew Chem Int Ed Engl *47*, 2253-2255.

Park, J.W., Vahidi, B., Taylor, A.M., Rhee, S.W., and Jeon, N.L. (2006). Microfluidic culture platform for neuroscience research. Nat Protoc *1*, 2128-2136.

Penningroth, S.M., Cheung, A., Bouchard, P., Gagnon, C., and Bardin, C.W. (1982). Dynein Atpase Is Inhibited Selectively in Vitro by Erythro-9-[3-2-(Hydroxynonyl)]Adenine. Biochem Biophys Res Commun *104*, 234-240.

Sotthibundhu, A., Sykes, A.M., Fox, B., Underwood, C.K., Thangnipon, W., and Coulson, E.J. (2008). β-amyloid$_{1-42}$ induces neuronal death through the p75 neurotrophin receptor. J Neurosci *28*, 3941-3946.

Stine, W.B., Jr., Dahlgren, K.N., Krafft, G.A., and LaDu, M.J. (2003). In vitro characterization of conditions for amyloid-β peptide oligomerization and fibrillogenesis. J Biol Chem *278*, 11612-11622.

Taylor, A.M., Blurton-Jones, M., Rhee, S.W., Cribbs, D.H., Cotman, C.W., and Jeon, N.L. (2005). A microfluidic culture platform for CNS axonal injury, regeneration and transport. Nat Methods *2*, 599-605.

Vohra, B.P., Sasaki, Y., Miller, B.R., Chang, J., DiAntonio, A., and Milbrandt, J. (2010). Amyloid precursor protein cleavage-dependent and -independent axonal degeneration programs share a common nicotinamide mononucleotide adenylyltransferase 1-sensitive pathway. J Neurosci *30*, 13729-13738.

Wang, F., Flanagan, J., Su, N., Wang, L.C., Bui, S., Nielson, A., Wu, X., Vo, H.T., Ma, X.J., and Luo, Y. (2012). RNAscope: a novel in situ RNA analysis platform for formalin-fixed, paraffin-embedded tissues. J Mol Diagn *14*, 22-29.

Wang, Y., Shen, J., Arenzana, N., Tirasophon, W., Kaufman, R.J., and Prywes, R. (2000). Activation of ATF6 and an ATF6 DNA binding site by the endoplasmic reticulum stress response. J Biol Chem *275*, 27013-27020.

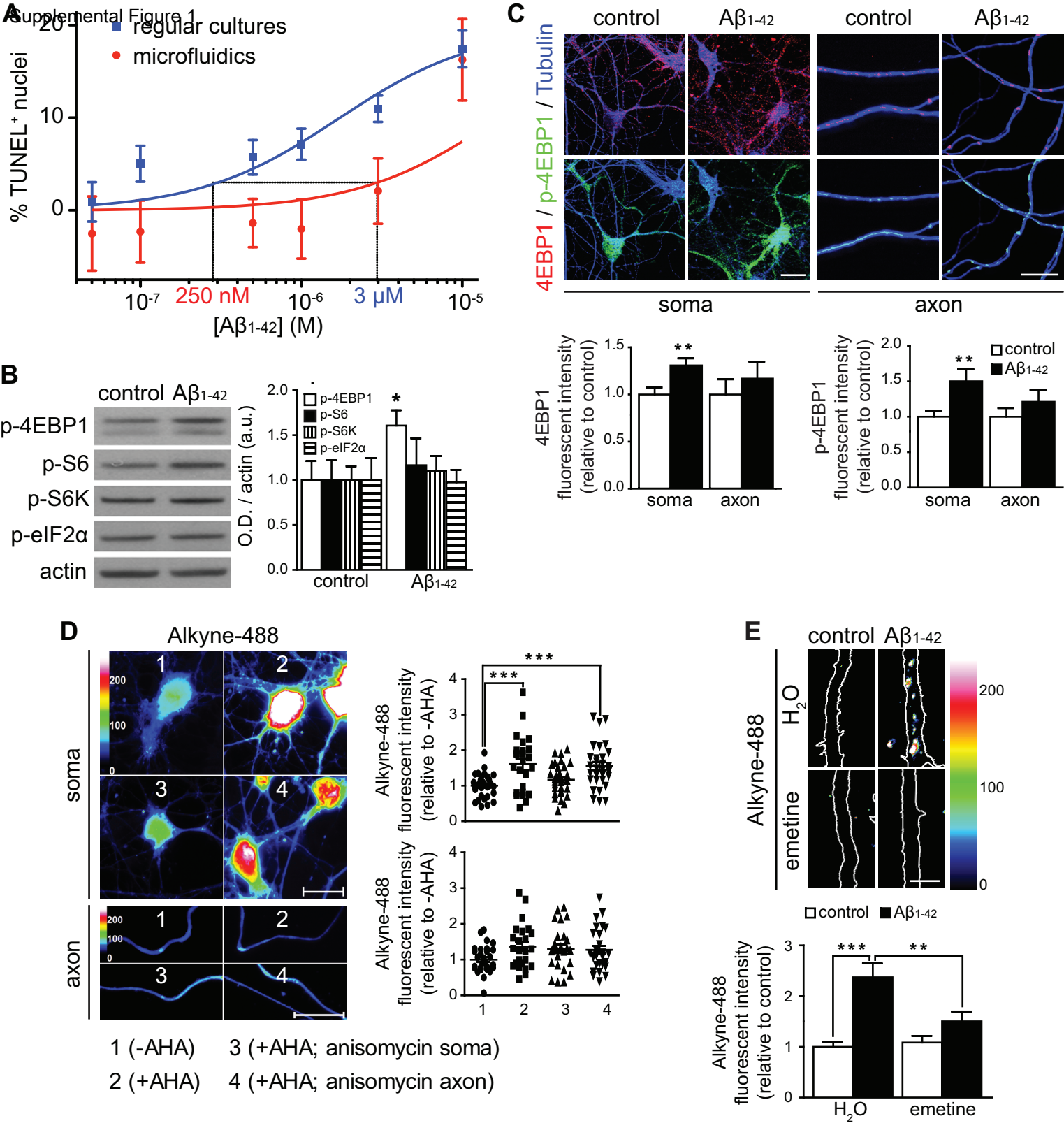
A
regular cultures
microfluidics
% TUNEL+ nuclei
20
10
0
10-7
250 nM
10-6
3 µM
10-5
[Aβ1-42] (M)
B
control
Aβ1-42
p-4EBP1
p-S6
p-S6K
p-eIF2α
actin
O.D. / actin (a.u.)
p-4EBP1
p-S6
p-S6K
p-eIF2α
control
Aβ1-42
C
control
Aβ1-42
control
Aβ1-42
4EBP1 / p-4EBP1 / Tubulin
soma
axon
4EBP1 fluorescent intensity (relative to control)
p-4EBP1 fluorescent intensity (relative to control)
control
Aβ1-42
soma
axon
D
Alkyne-488
soma
axon
1
2
3
4
Alkyne-488 fluorescent intensity (relative to -AHA)
1 (-AHA)
2 (+AHA)
3 (+AHA; anisomycin soma)
4 (+AHA; anisomycin axon)
E
control
Aβ1-42
Alkyne-488
H2O
emetine
control
Aβ1-42
Alkyne-488 fluorescent intensity (relative to control)
H2O
emetine

Figure S1

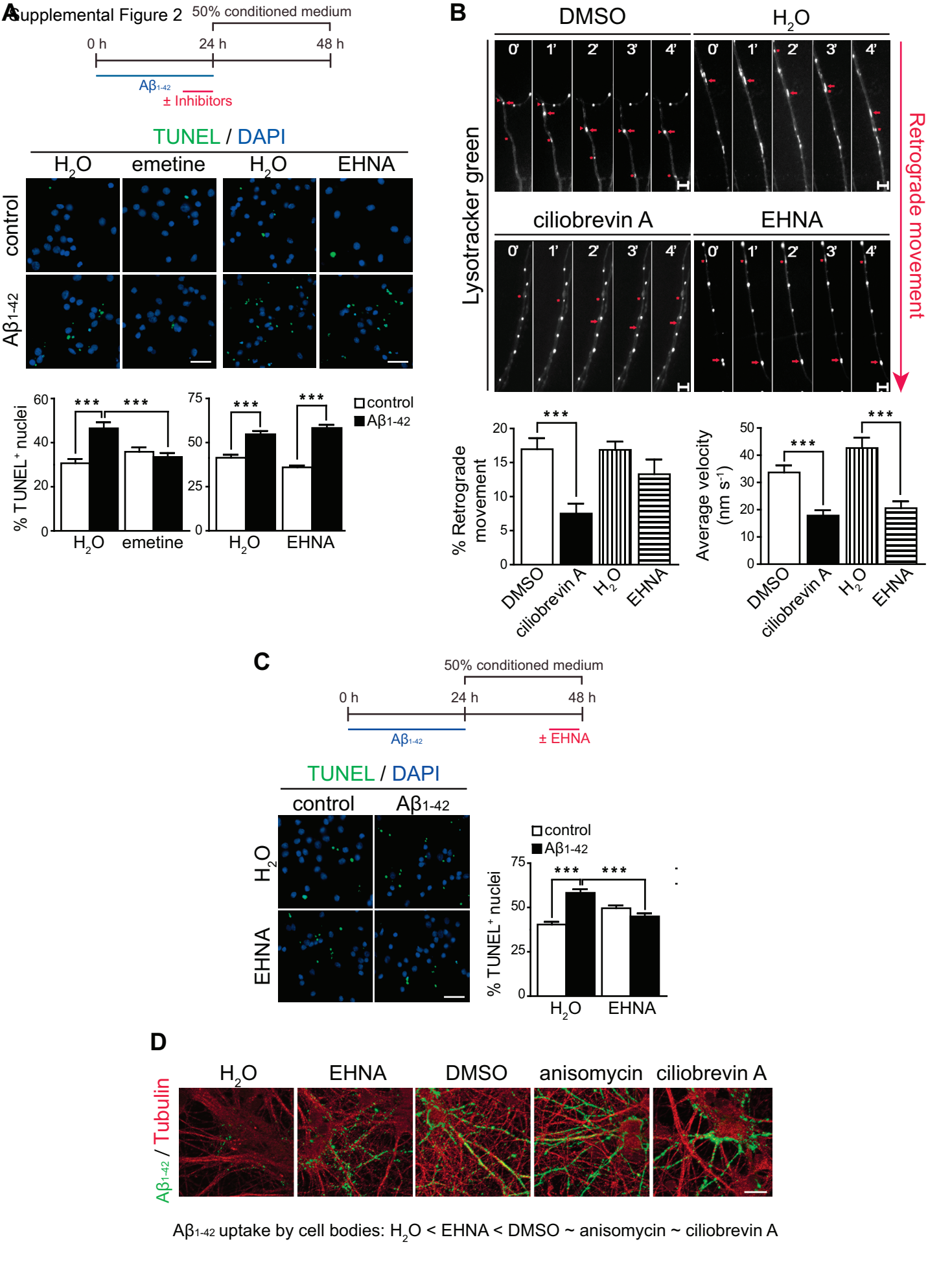
Supplemental Figure 2
A
50% conditioned medium
0 h
24 h
48 h
Aβ1-42
± Inhibitors
TUNEL / DAPI
H2O
emetine
H2O
EHNA
control
Aβ1-42
% TUNEL+ nuclei
control
Aβ1-42
B
DMSO
H2O
ciliobrevin A
EHNA
Lysotracker green
Retrograde movement
% Retrograde movement
Average velocity (nm s-1)
C
50% conditioned medium
0 h
24 h
48 h
Aβ1-42
± EHNA
TUNEL / DAPI
control
Aβ1-42
H2O
EHNA
% TUNEL+ nuclei
D
H2O
EHNA
DMSO
anisomycin
ciliobrevin A
Aβ1-42 / Tubulin
Aβ1-42 uptake by cell bodies: H2O < EHNA < DMSO ~ anisomycin ~ ciliobrevin A

Figure S2

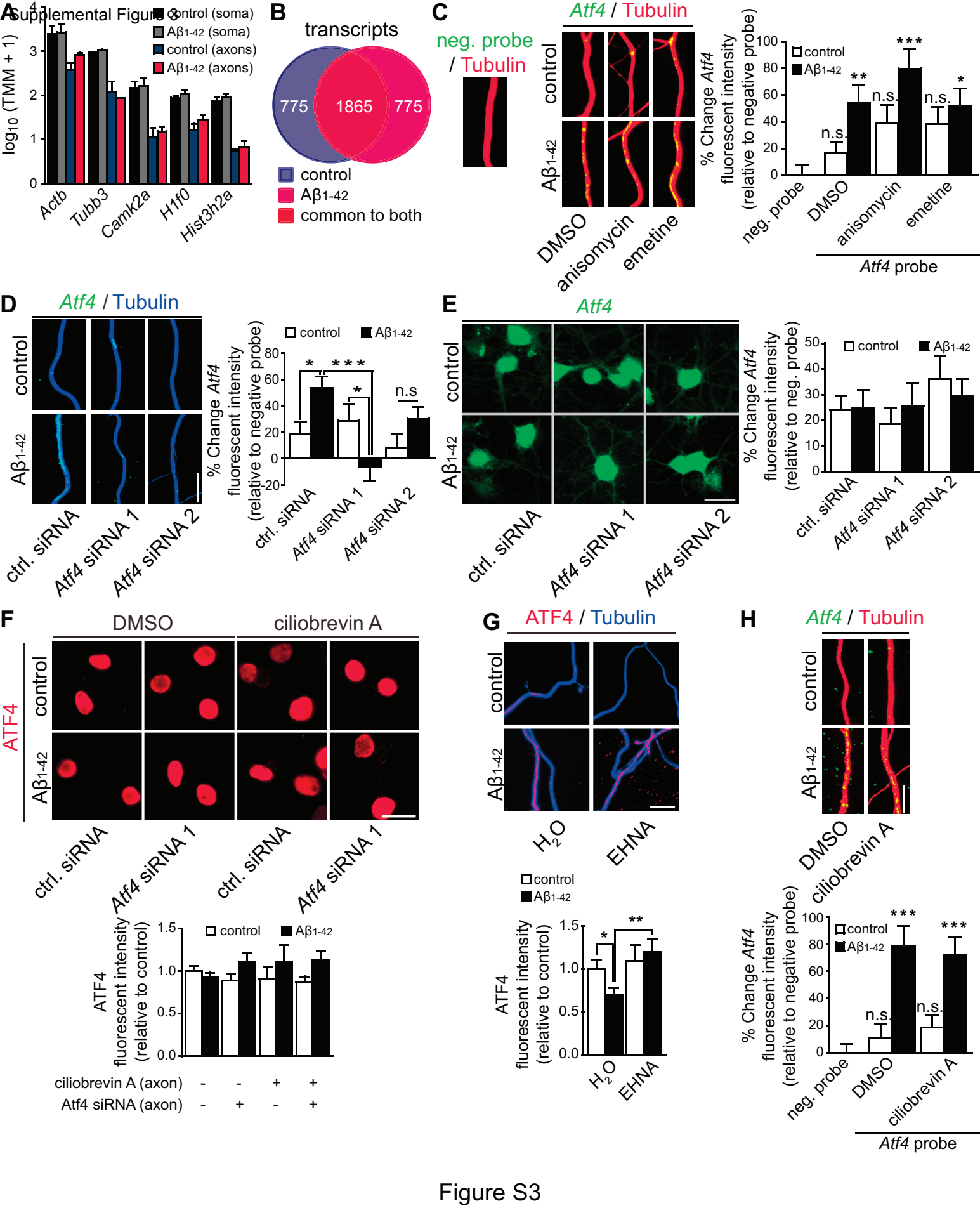
Supplemental Figure 3
A
control (soma)
Aβ1-42 (soma)
control (axons)
Aβ1-42 (axons)
log10 (TMM + 1)
Actb
Tubb3
Camk2a
H1f0
Hist3h2a
B
transcripts
775
1865
775
control
Aβ1-42
common to both
C
Atf4 / Tubulin
neg. probe / Tubulin
control
Aβ1-42
DMSO
anisomycin
emetine
% Change Atf4 fluorescent intensity (relative to negative probe)
neg. probe
Atf4 probe
D
Atf4 / Tubulin
ctrl. siRNA
Atf4 siRNA 1
Atf4 siRNA 2
% Change Atf4 fluorescent intensity (relative to negative probe)
n.s
E
Atf4
% Change Atf4 fluorescent intensity (relative to neg. probe)
F
DMSO
ciliobrevin A
ATF4
ATF4 fluorescent intensity (relative to control)
ciliobrevin A (axon)
Atf4 siRNA (axon)
G
ATF4 / Tubulin
H2O
EHNA
H
Atf4 / Tubulin

Figure S3

Supplemental Figure 4

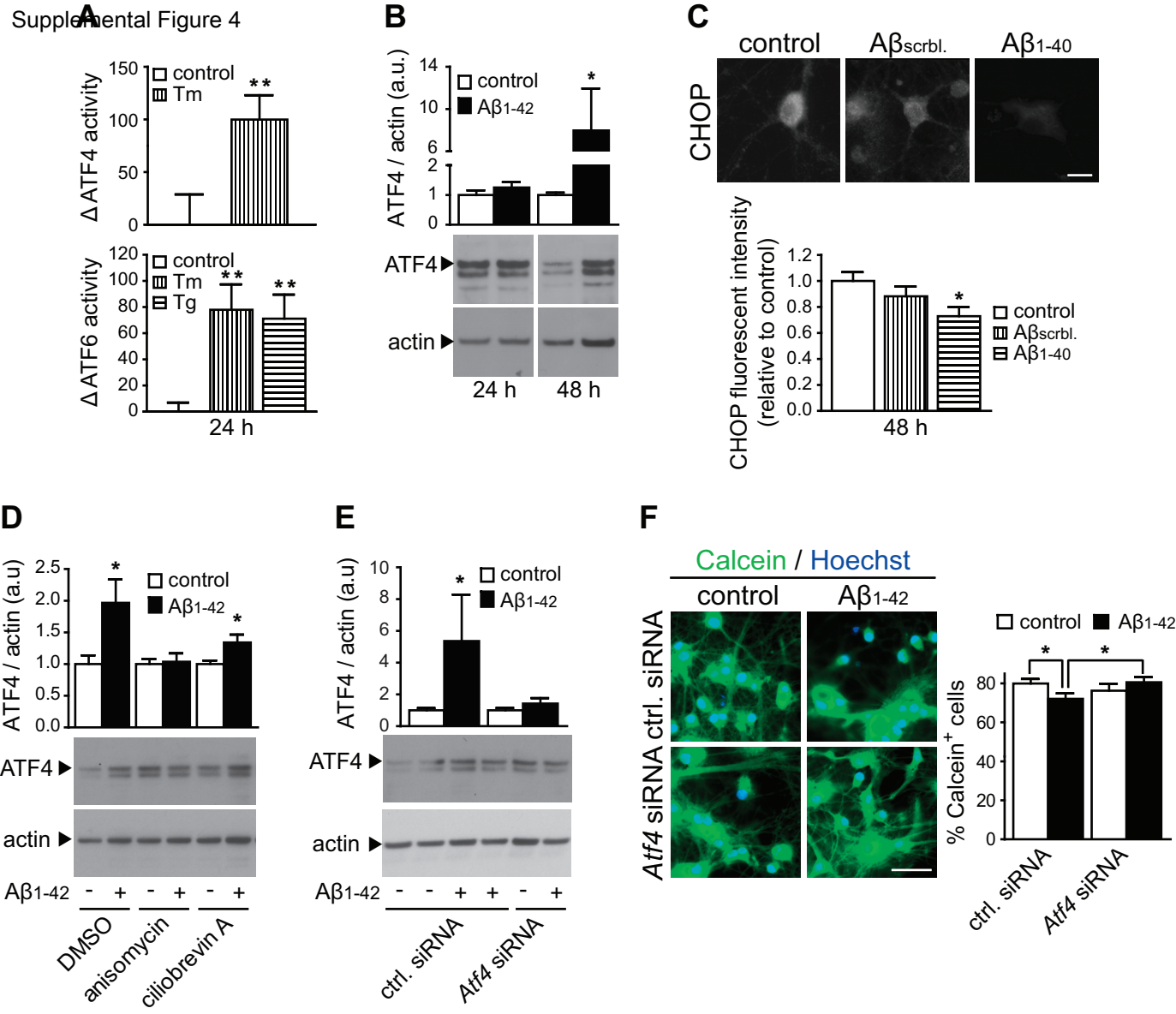

Figure S4

Supplemental Figure 5

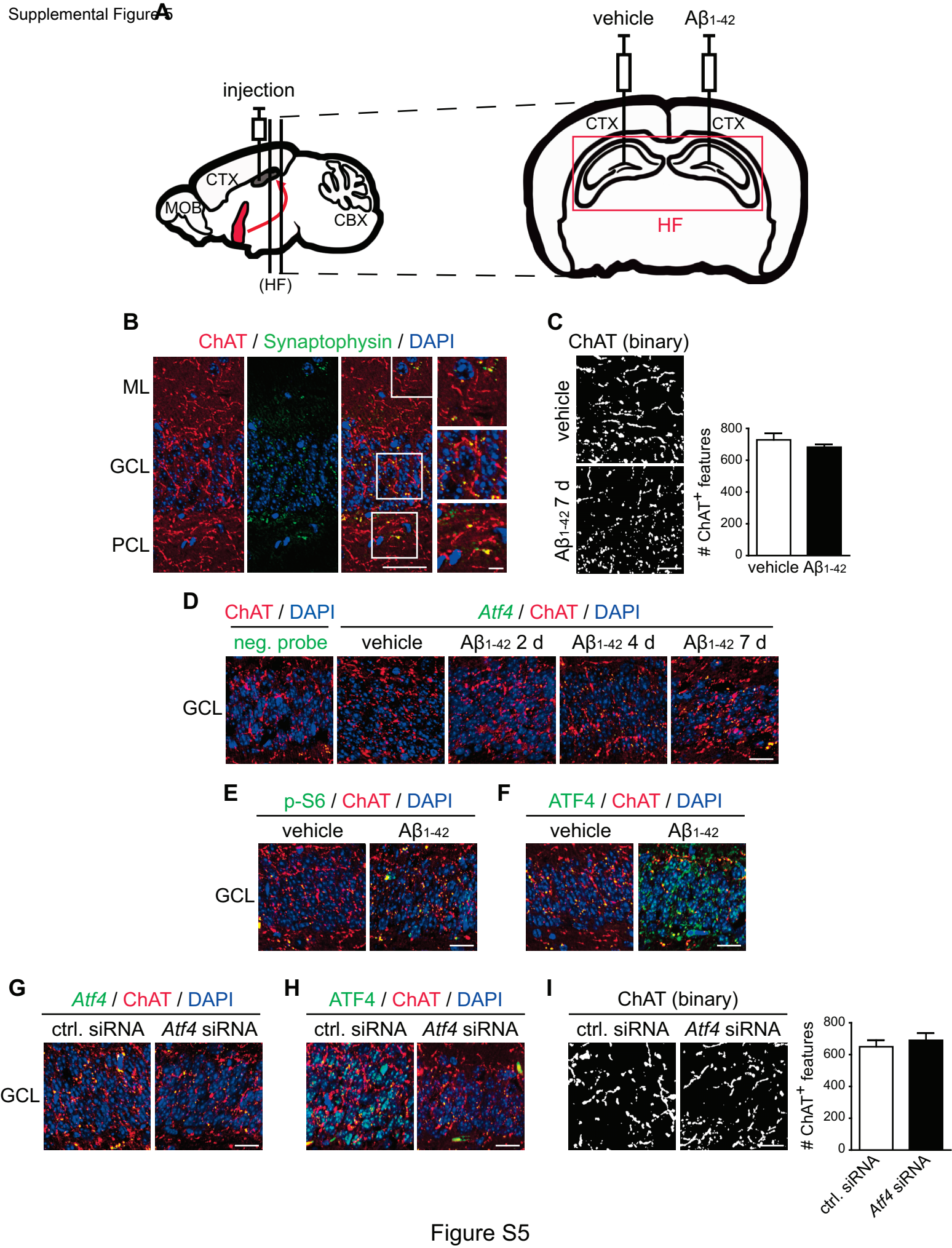

Figure S5

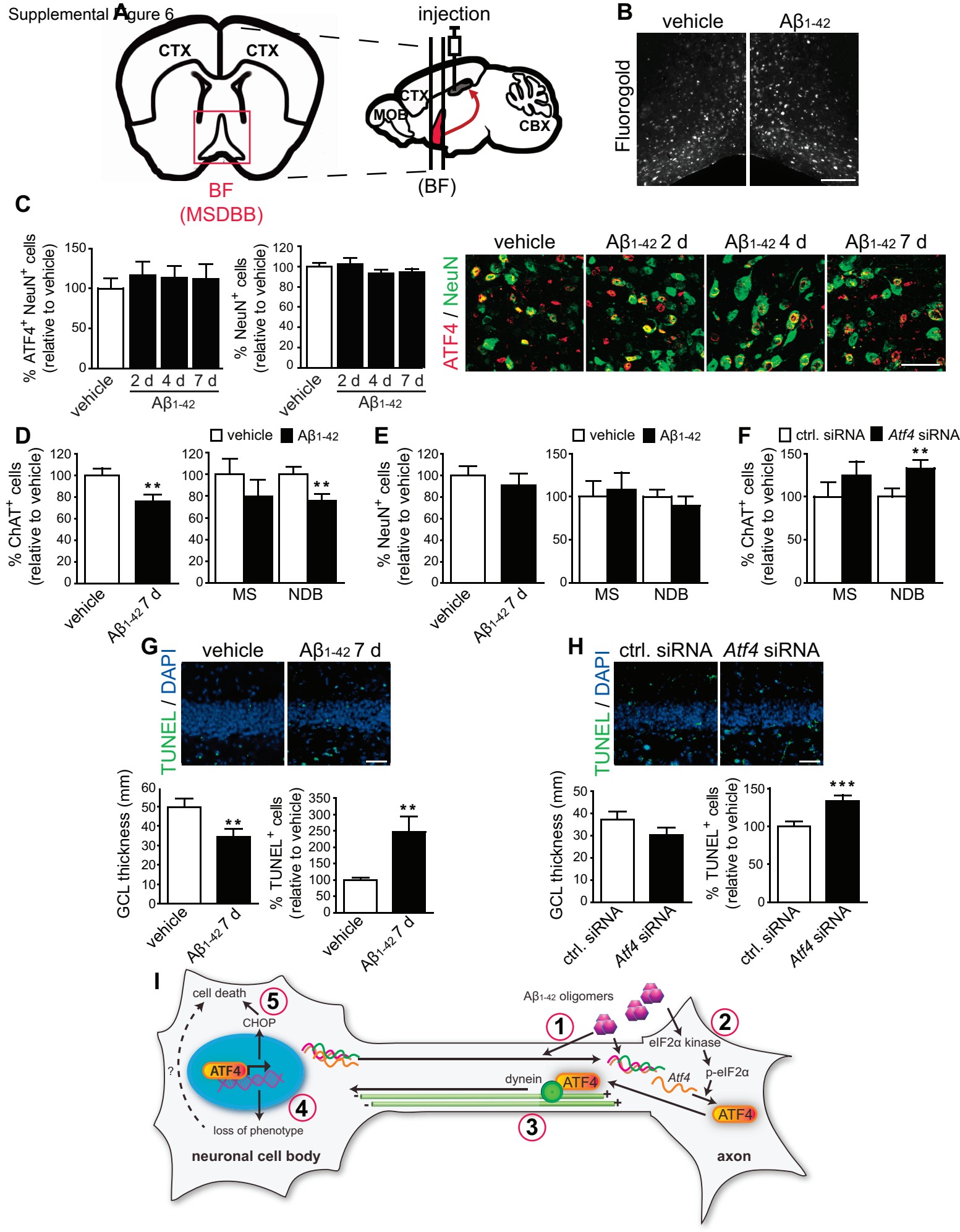
A
injection
CTX
CTX
CTX
MOB
CBX
BF
(MSDBB)
(BF)
B
vehicle
Aβ1-42
Fluorogold
C
% ATF4+ NeuN+ cells (relative to vehicle)
% NeuN+ cells (relative to vehicle)
vehicle
2 d
4 d
7 d
Aβ1-42
vehicle
Aβ1-42 2 d
Aβ1-42 4 d
Aβ1-42 7 d
ATF4 / NeuN
D
% ChAT+ cells (relative to vehicle)
vehicle
Aβ1-42
Aβ1-42 7 d
MS
NDB
E
% NeuN+ cells (relative to vehicle)
F
ctrl. siRNA
Atf4 siRNA
G
TUNEL / DAPI
vehicle
Aβ1-42 7 d
GCL thickness (mm)
% TUNEL+ cells (relative to vehicle)
H
ctrl. siRNA
Atf4 siRNA
I
cell death
5
CHOP
ATF4
?
4
loss of phenotype
neuronal cell body
Aβ1-42 oligomers
1
2
eIF2α kinase
Atf4
p-eIF2α
dynein
ATF4
3
ATF4
axon

Figure S6